Journal of Biomechanics 45 (2012) 99–106

Contents lists available at SciVerse ScienceDirect

Journal of Biomechanics

journal homepage: www.elsevier.com/locate/jbiomech
www.JBiomech.com

Kinetics of the cervical spine in pediatric and adult volunteers during low speed frontal impacts

Thomas Seacrist [a,*], Kristy B. Arbogast [a,f], Matthew R. Maltese [c], J. Felipe García-España [a], Francisco J. Lopez-Valdes [d], Richard W. Kent [d], Hiromasa Tanji [e], Kazuo Higuchi [e], Sriram Balasubramanian [a,b]

[a] Center for Injury Research and Prevention, The Children's Hospital of Philadelphia, USA
[b] School of Biomedical Engineering, Science and Health Systems, Drexel University, USA
[c] Department of Anesthesiology and Critical Care Medicine, The Children's Hospital of Philadelphia, USA
[d] Center for Applied Biomechanics, University of Virginia, USA
[e] Takata Corporation, Japan
[f] Dept of Pediatrics, University of Pennsylvania, USA

ARTICLE INFO

Article history:
Accepted 28 September 2011

Keywords:
Kinetics
Inverse dynamics
Pediatrics
ATD

ABSTRACT

Previous research has quantified differences in head and spinal kinematics between children and adults restrained in an automotive-like configuration subjected to low speed dynamic loading. The forces and moments that the cervical spine imposes on the head contribute directly to these age-based kinematic variations. To provide further explanation of the kinematic results, this study compared the upper neck kinetics – including the relative contribution of shear and tension as well as flexion moment – between children ($n=20$, 6–14 yr) and adults ($n=10$, 18–30 yr) during low-speed (<4 g, 2.5 m/s) frontal sled tests. The subjects were restrained by a lap and shoulder belt and photo-reflective targets were attached to skeletal landmarks on the head, spine, shoulders, sternum, and legs. A 3D infrared tracking system quantified the position of the targets. Shear force (F_x), axial force (F_z), bending moment (M_y), and head angular acceleration ($\ddot{\theta}_{head}$) were computed using inverse dynamics. The method was validated against ATD measured loads. Peak F_z and $\ddot{\theta}_{head}$ significantly decreased with increasing age while M_y significantly increased with increasing age. F_x significantly increased with age when age was considered as a univariate variable; however when variations in head-to-neck girth ratio and change in velocity were accounted for, this difference as a function of age was not significant. These results provide insight into the relationship between age-based differences in head kinematics and the kinetics of the cervical spine. Such information is valuable for pediatric cervical spine models and when scaling adult-based upper cervical spine tolerance and injury metrics to children.

1. Introduction

Understanding the forces and moments the cervical spine imposes on the head for a restrained occupant provides insight into how the restraint forces applied to the torso translate into the occupant's head and spinal kinematics. In human subjects in simulated crashes, however, cervical spine reaction forces and moments cannot be measured directly. To address this limitation, researchers have reported methods for calculating loads and moments at the upper cervical spine in adult human volunteers and post mortem human subjects (PMHS) by transforming accelerations measured externally on the head to the center of gravity of the head using standard dynamics equations (Mertz and Patrick, 1967; Ewing and Thomas, 1973; Sundararajan et al., 2004; Funk et al., 2009). Using these approaches, adult head and neck forces and moments have been reported in low-speed rear impacts (Howard et al., 1998; Ono et al., 1997; Vijayakumar et al., 2006) and frontal loading at various speeds (Lopez-Valdes et al., 2010a; Wismans et al., 1986). However, similar studies involving pediatric subjects are completely absent from the literature.

It is well documented that the structure of the cervical spine changes with maturation suggesting that the spinal kinetics may also vary with age. In the first few years of life, the cervical vertebrae fuse and uncovertebral joints on the lateral contours of the vertebrae form but are not complete until approximately 6 years of age (Cattell and Filtzer, 1965; Fuchs et al., 1989; Janssen et al., 1991; Kriss and Kriss, 1996; Schuer and Black, 2000; Weber, 2002; Yoganandan et al., 2002). Changes continue throughout the pediatric age range until the early teenage years. Kasai et al. (1996) documented an increase in

* Correspondence to: Center for Injury Research and Prevention, Children's Hospital of Philadelphia, 3535 Market St, Suite 1150, PA 19104, USA.
Tel.: +1 267 426 5432; fax: +1 215 590 5425.
E-mail address: seacrist@email.chop.edu (T. Seacrist).

0021-9290/$ - see front matter © 2011 Elsevier Ltd. All rights reserved.
doi:10.1016/j.jbiomech.2011.09.016

vertebral body diameter from age 10–14 years, an increase in the initially horizontal facet angle through age 10 years (likely limiting risk of subluxation with increasing age), and changes in the cervical lordosis angle (angle between C3–C7) through the ages of puberty. The thoracic kyphotic angle (angle between T4–T9) has been reported to decrease until approximately 10 years and then increase through young adulthood (McGowan et al., 1995). Based on these structural changes with maturation, we hypothesize that the kinetics of the cervical spine and subsequent kinematics of the head of a restrained occupant will change with age.

Previous research highlighted kinematic differences in the head and spine between children and adults using simulated low-speed frontal crashes with human volunteers restrained in an automotive-like configuration (Arbogast et al., 2009). Briefly, the normalized forward excursion of the head and spine significantly decreased with age and all spinal markers moved upward due to a combination of rigid body rotation and spinal flexion with less upward movement with age. The majority of the spine flexion occurred at the base of the neck, not in the upper cervical spine and the magnitude of flexion was greatest for the youngest subjects. We hypothesize that these kinematic differences are related to kinetic differences in the cervical spine across age. Therefore, the objective of this study was to quantify the age-related differences in the upper neck shear force, axial force, and bending moment of restrained human volunteers in low-speed frontal loading.

2. Methods

This study protocol was reviewed and approved by the Institutional Review Boards at The Children's Hospital of Philadelphia, Philadelphia, PA and Rowan University, Glassboro, NJ.

2.1. Human volunteer instrumentation, testing, and data processing

A comprehensive description of the testing method can be found in Arbogast et al. (2009). Briefly, low-speed frontal sled tests were conducted using 20 pediatric (6–14 years) and 10 adult (18–30 years) male human volunteers. A pneumatically actuated, hydraulically controlled low-speed acceleration sled (Fig. 1) consisting of a moving platform with a low back padded seat, mock B-pillar, fixed lap belt anchors, and an adjustable foot rest was designed to subject restrained human volunteers to a sub-injurious, low-speed frontal crash pulse. Subjects were restrained using an automotive three-point belt system consisting of a retractor with automatic locking retractor function and cinching latch plate. The height of the shoulder belt anchor was adjusted to provide similar fit across subjects; specifically, the shoulder belt angle at the D-Ring and the lab belt buckle angle were set at 70° at initial position for all the subjects.

Informed consent was obtained from all adult volunteers or a legal guardian for pediatric volunteers. Informed assent was obtained from pediatric volunteers. Several anthropometric measurements were obtained from the subjects prior to testing (Table 1). Photo-reflective targets were placed on anatomical landmarks including the head, spine, shoulders, sternum, and legs and tracked using a 3D motion analysis system at 100 Hz (Model Eagle 4, Motion Analysis Corporation, Santa Rosa, CA). Subjects received six consecutive trials. No subjects experienced any injuries or complained of lingering pain. Additionally, three trials were performed on an instrumented Hybrid III 6-year-old (H36) anthropomorphic test device (ATD) to validate the inverse dynamics method. Validation results are described in Appendix.

Signals from the accelerometers, angular rate sensor (ARS), and load cells were sampled at 10,000 Hz using a T-DAS data acquisition system (Diversified Technical Systems Inc., Seal Beach, CA). The time series motion analysis and T-DAS data were imported into MATLAB (Mathworks, Inc., Natick, MA) for inverse dynamics calculations using a custom written program.

2.2. Inverse dynamics

Forces and moment of the upper neck acting on the head were calculated based on the motion analysis data using two-dimensional inverse dynamics

Table 1
Measured anthropomorphic data.

Age (yr)	Head				Neck			
	Width (cm)	Depth (cm)	Length (cm)	Girth (cm)	Width (cm)	Depth (cm)	Length (cm)	Girth (cm)
6	14.2	18.5	21.0	53.2	8.7	7.6	16.0	25.4
7	13.4	19.0	21.5	52.7	8.4	7.5	14.0	26.1
7	14.2	16.8	20.5	52.5	8.6	7.5	17.0	28.0
8	15.2	19.1	21.2	54.0	9.5	7.7	15.1	29.0
8	14.4	18.7	20.9	54.5	8.2	8.0	16.0	29.0
9	14.4	18.6	21.3	52.6	8.1	7.1	14.5	26.9
10	14.4	17.5	19.6	51.2	8.3	7.3	15.5	27.5
10	14.0	18.6	21.4	53.0	8.4	7.7	16.0	28.0
10	14.2	17.8	20.4	51.5	9.1	8.5	13.0	29.5
11	14.2	18.7	20.3	54.5	10.0	8.0	16.0	31.3
11	13.9	18.1	20.5	53.2	8.6	7.8	16.0	28.5
12	14.8	19.1	22.3	55.1	9.3	8.7	18.5	30.5
12	15.0	19.8	21.8	58.5	10.0	8.6	17.5	34.0
12	14.4	18.5	21.9	54.0	8.8	9.0	17.0	32.0
12	14.3	18.2	20.8	54.0	9.4	8.7	15.5	31.0
13	15.0	18.4	20.9	54.0	9.6	9.0	18.5	32.0
13	15.2	19.3	22.2	55.5	9.9	9.3	17.5	30.5
13	15.7	19.7	23.3	57.5	11.8	10.6	19.0	36.5
13	14.7	18.5	21.3	53.7	10.0	9.0	16.5	33.0
14	15.0	20.5	23.8	58.5	10.7	10.2	17.0	37.0
18	15.9	19.7	23.2	59.0	11.2	10.2	20.0	39.5
19	16.0	20.0	23.1	60.3	12.5	11.2	19.0	39.5
20	15.9	20.2	24.4	59.5	13.1	11.2	20.0	42.0
22	16.0	19.7	23.5	57.1	11.3	10.6	17.0	38.3
22	16.0	20.3	22.5	60.5	11.9	11.3	19.7	39.5
22	15.9	20.6	24.9	59.9	13.5	12.6	18.5	44.1
22	14.5	18.3	21.5	55.0	11.3	10.0	14.5	37.0
24	15.3	19.0	23.0	57.5	11.8	10.8	19.2	37.9
24	15.1	19.3	22.5	57.0	11.9	11.8	18.5	38.0
30	15.4	20.7	24.2	58.5	11.7	11.0	18.5	40.1

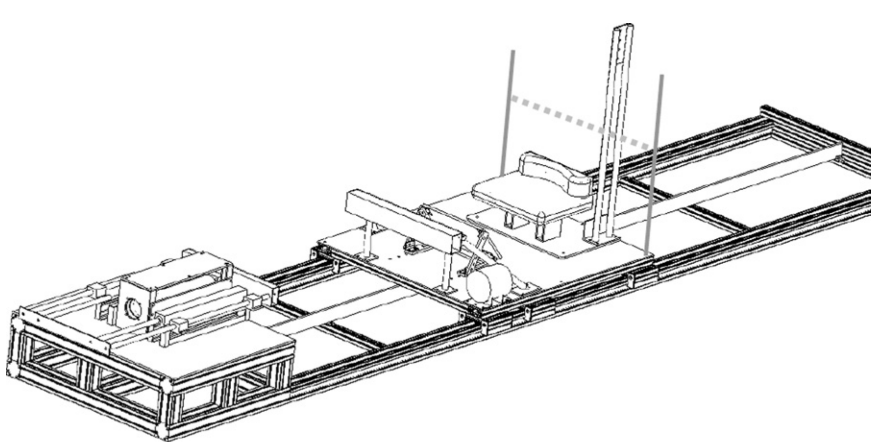

Fig. 1. Schematic of low-speed acceleration sled.